# Identifying Age-related Macular Degeneration In Volumetric Retinal Images

Abdulrahman Albarrak [a], Frans Coenen [a] and Yalin Zheng [b]

[a] Department of Computer Science, Ashton Building, University of Liverpool, Liverpool
[b] Department of Eye and Vision Science, University of Liverpool, Liverpool, UK

## ABSTRACT

Age-related Macular Degeneration (AMD) is a retina disorder, which is currently on the increase. In this paper, we investigate the use two different statistical methods for detecting AMD in Optical Coherence Tomography (OCT) volumetric data where by a 3-D image is represented using a combination of two matrices: a Voxel Co-occurrence Matrix (VCM) and a Voxel Run-Length Matrix (VRLM). Statistical features are extracted from the matrices which are then used to establish feature vectors for input to a standard classification (The k-nearest neighbor (KNN) classifier was used in this paper).

**Keywords:** Gray Level Co-occurrence Matrices, texture analysis, Feature Vector, Statistical Feature Extraction, Grey Level Run-Length Matrices, KNN, AMD, OCT, retina

## 1. OVERVIEW

Optical Coherence Tomography (OCT) is an imaging technology that is able to build a three-dimensional images of the retina such that different retina layers can be distinguished [1]. The use of OCT enhances the support available for the examination of different eye disorders. Age-related Macular Degeneration(AMD) is one of these disorders. OCT images indicate clearly different signs of AMD. Figure 1 shows two sequences taken from OCT volumes. The sequence on the left shows a normal retina, and the sequence on the right a retina effected by AMD.

There is very little published work on the classification of 3D OCT images. Most of the research on the classification of retinal images has been at 2D images representing the "fovea slice" of an OCT volume [2]. However, the main disadvantage of these 2D methods is that in some cases the signs of a retina disorder may appear in some other slices and not in the fovea slice. The technique described in this paper uses the entire 3-D OCT volume.

There are three main steps for our technique. First of all, the image features are extracted by the means of a combination of texture methods acting as shape descriptors. Two different matrices are used for this purpose, (i) a Voxel Co-occurrence Matrix (VCM) and (ii) a Voxel Run-Length Matrix (VRLM). Following this, various statistical features are computed using these matrices. With respect to 2-D images, the work described in [3] introduced 14 statistical textural features such as angular second moment, contrast, correlation, variance and others. It is noticeable that different extracted features could be used with one matrix but it might not be suitable with other. The extracted features are then used to populate a set of Feature Vectors (FVs), one per image. The final step is to input the FVs into a classification system. Different classifiers could be used. K-nearest neighbor (KNN) was selected with respect to this paper because of its wide usage.

## 2. FEATURE REPRESENTATION AND EXTRACTION

In order to reduce the dimensionality of the volumetric images, two matrices are used: (i) a Voxel Co-occurrence Matrix (VCM) and (ii) a Voxel Run-Length Matrix (VRLM). These matrices consider the neighboring relationships between the volume elements (voxels). The use of these kind of matrices reduce the dimensionality by considering only the relationships between the image elements. After computing these matrices, features are extracted from the two matrices. The VCM and VRLM matrices are considered in more detail in the following two sub-sections.

Further author information: (Send correspondence to Abdulrahman Albarrak)
Abdulrahman Albarrak: E-mail: A.Albarrak@liverpool.ac.uk

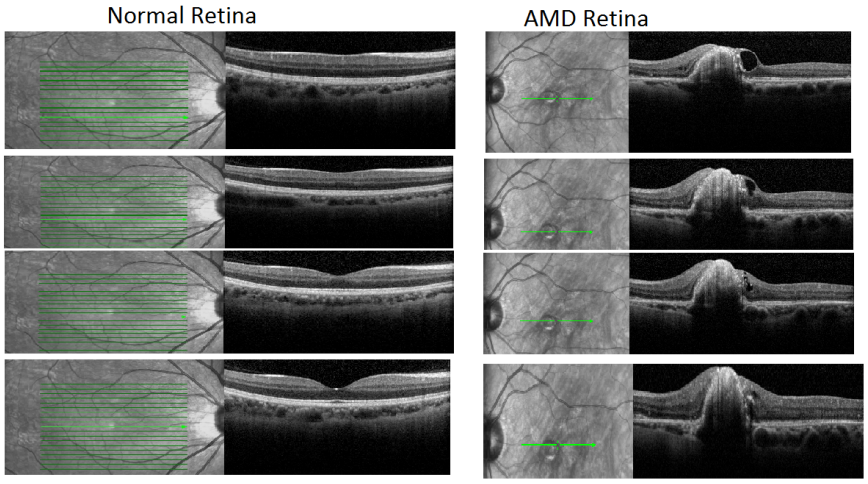


Figure 1. Four slices in the same locations for a normal retina and one with AMD signs. In every slice, the left hand side shows the fundus images with an arrow indicating the position of the OCT scanning.

## 2.1 VCM

The idea of the VCM matrix is founded on the concept of the Grey Level Co-occurrence Matrix (GLCM) used with 2D images [3]. The basic idea of the GLCM matrix is to count the number of pairs pixel, that display the same attributes, located within a certain distant and a direction of each other. A GLCM matrix when generated holds the frequencies of neighboring pixel intensity values calculated by using the second-order conditional probability functions. Many GLCMs could be computed from the same data by varying the distance and the direction.

In 2-D images we can identify four directions, in the case of 3-d images we can identify 13 vectors. The Voxel Co-occurrence Matrices (VCM) for 3D objects [4] is defined as follows: VCM(i, j | d, $\Phi$, $\theta$)= #((l, m, n),(o, p, q)) $\epsilon(L_x \times L_y \times L_z)$ I (l, m, n)= i, I (o, p, q) = j , where d is the displacement distance , $\Phi$ and $\theta$ are the angles displacement angle for j, # indicates the frequency of an intensity pair, $L_x$ =1, 2 ... $N_x$, $L_y$=1, 2 ... , $N_y$, $L_z$=1, 2 ..., $N_z$ are the horizontal (X), vertical (Y), depth (Z) values of the image intensity and I is the volumetric image. For simplicity, the value of d could be set to one [3]. The value of $\theta$ could be 0, 45, 90 and 135 in 2D cases while in 3D cases 54.7 and 125.3 should be included.

All 13 vectors were used and for every vector a VCM matrix was built consequently 13 VCMs were generated(one per image). In order to illustrate how to form the matrices. Let $d$ be the displacement vector used in $\delta = (\Delta x, \Delta y, \Delta z)$, VCMs could be defined using the 13 vectors involving in table 1. This table shows the possible displacement vectors in both ways(minus and pulse). For example, $\pm(d, 0, 0)$ vector indicates that the selected element is increased by the value $d$ in $x$ direction in both way. The angle $\Phi$ represents the change in azimuth direction and the angle $\theta$ is for zenith, which are the vertical and horizontal coordinates respectively (See Figure 2).

After computing the VCM matrix, the followings are features that are used [3,6]:

- Angular Second moment: $f_1 = \sum_i \sum_j VCM(i,j)^2$
- Contrast: $f_2 = \sum_{n=0}^{N_g} n^2 \left\{ \sum_{i=1}^{N_g} \sum_{j=1}^{N_g} VCM(i,j) \right\}$ , where $|i-j|= n$
- Correlation: $f_3 = \frac{\sum_i \sum_j (ij) VCM(i,j) - \upsilon_x \upsilon_y}{\sigma_x \sigma_y}$, where $\upsilon_x$, $\upsilon_y$, $\sigma_x$ and $\sigma_y$ are the means, standard deviations of the matrix elements respectively.
- Sum of squares (Variance): $f_4 = \sum_i \sum_j (i-\upsilon)^2 VCM(i,j)$

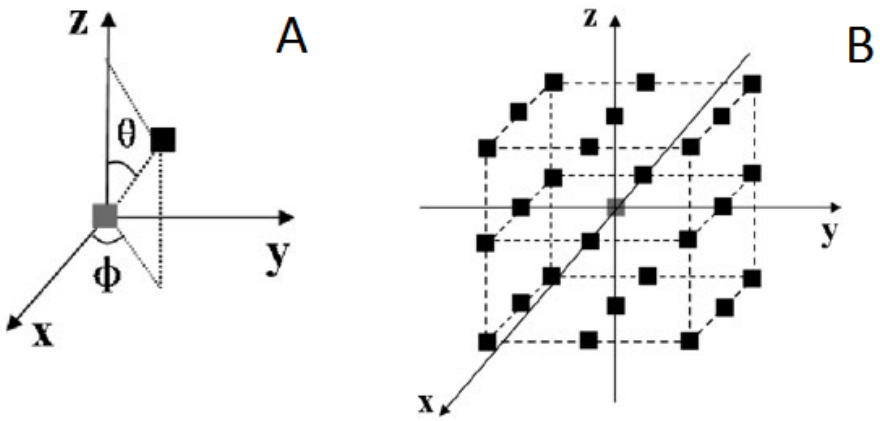


Figure 2. Illustration of the relationships between the angles within the 3D images. (a) illustrates the angle $\Phi$ and $\theta$ while (b) shows a single voxel and its possible 26 neighbors [5].

Table 1. The possible 13 displacement vectors [5].

| Displacement value (D) | Direction ($\Phi$, $\theta$) |
|---|---|
| $\pm(d,0,0)$ | $(0,90)$ |
| $\pm(0,d,0)$ | $(90,90)$ |
| $\pm(0,0,d)$ | $(0,90)$ |
| $\pm(d,d,0)$ | $(45,90)$ |
| $\pm(-d,d,0)$ | $(135,90)$ |
| $\pm(0,d,d)$ | $(90,45)$ |
| $\pm(0,d,-d)$ | $(90,135)$ |
| $\pm(d,0,d)$ | $(0,45)$ |
| $\pm(d,0,-d)$ | $(0,135)$ |
| $\pm(d,d,d)$ | $(45,54.7)$ |
| $\pm(-d,d,d)$ | $(135,54.7)$ |
| $\pm(d,d,-d)$ | $(54,125.3)$ |
| $\pm(-d,d,-d)$ | $(135,125.3)$ |

- Inverse Difference Moment: $f_5 = \sum_i \sum_j \frac{1}{1+(i-j)^2} VCM(i,j)$
- Sum Average: $f_6 = \sum_{i=2}^{2N_g} iVCM_{x+y}(i)$
- Sum Variance: $f_7 = \sum_{i=2}^{2N_g} (i-f_8)^2 VCM_{x+y}(i)$
- Sum Entropy: $f_8 = \sum_{i=2}^{2N_g} VCM_{x+y}(i) \log VCM_{x+y}(i)$
- Entropy: $f_9 = -\sum_i \sum_j VCM(i,j) \log(VCM(i,j))$
- Difference Entropy: $f_{10} = \sum_{i=0}^{N_{g-1}} VCM_{x-y} \log VCM_{x-y}(i)$
- Different Variance: $f_{11}$ =variance of $VCM_{x-y}$
- Maximal Correlation Coefficient: $f_{12}$=(second eigenvalue of Q)$^{1/2}$, where Q(i, j)=$\sum_k \frac{VCM(i,k)VCM(j,k)}{VCM_x(i)VCM_y(k)}$

- Information Measures of Correlation: $f_{13} = \frac{f_9 - XY1}{\max(HX,HY)}$, $f_{14} = (1 - \exp[-2.0(XY2 - f_9)^{1/2}])$ where HX and HY are the entropies of $p_x$ and $VCM_y$ and $XY1 = -\sum_i \sum_j VCM(i,j) \log) \{VCM_x(i)VCM_y(j)\}$ and $XY2 = -\sum_i \sum_j VCM_x(i)VCM_y(j) \log) \{VCM_x(i)VCM_y(j)\}$

where P is the probability matrix, $N_g$ is the maximum value included in intensity values of the image.

More features could be included. The following lists some more statistical methods [7]:

- Dissimilarity: $f_{15} = \sum_i \sum_j |(i-j)| VCM(i,j)$
- Inverse difference: $f_{16} = \sum_i \sum_j \frac{1}{1+(i-j)} VCM(i,j)$
- Maximum probability: $f_{17} = \max$ (VCM(i, j)) $\forall$ i, j
- Inverse difference normalized: $f_{18} = \sum_i \sum_j \frac{VCM(i,j)}{1+|i-j|^2/N_g^2}$
- Inverse difference moment normalized: $f_{19} = \sum_i \sum_j \frac{VCM(i,j)}{1+(i-j)^2/N_g^2}$

In addition, autocorrelation and cluster features are used for VCM and the following is the method of computing them [8]:

- Autocorrelation: $f_{20} = \sum_i \sum_j (ij) VCM(i,j)$
- Cluster Shade: $f_{21} = \sum_i \sum_j (i + j - \mu_x - \mu_y)^3 VCM(i,j)$
- Cluster Prominence: $f_{22} = \sum_i \sum_j (i + j - \mu_x - \mu_y)^4 VCM(i,j)$

The previous 22 feature functions are applied for every VCM. 286 features are extracted by using VCMs for one image.

## 2.2 VRLM

The concept of the VRML matrix is founded on the Grey Level Run-Length Matrix (GLRLM) which is used to hold a gray level run elements in different lengths. A run is a set of consecutive, collinear image intensity pixels that have the same values. The length of the run is the number of intensity values in the run. The GLRLM(i, j) should include a run of length j in a certain direction involving a gray intensity level i [9, 10]. The Voxel Run-Length Matrix (VRLM) is a volumetric extension to the GLRLM.

The following function illustrates how to create a VRLM. $VRLM(\theta, \Phi) = [g(i,j|\theta,\Phi)], 0 \leq i \leq N_g, 0 \leq j \leq N_r$ where $\theta, \Phi$ are the angles as in the previous section, $g(i,j|\theta,\Phi)$ is the function for computing the run intensity of i with a length j in the two angles, $N_g$ is the number of voxels intensity levels in the image and $N_r$ is the maximum run length. Table 1 summaries the 13 possible vectors and the angles.

Five features were extracted from each matrix [9].

- Short Runs Emphasis: $f_1 = \sum_{i=1}^{N_g} \sum_{j=1}^{N_r} \frac{VRLM(i,j)}{j^2} / \sum_{i=1}^{N_g} \sum_{j=1}^{N_r} VRLM(i,j)$
- Long Runs Emphasis: $f_2 = \sum_{i=1}^{N_g} \sum_{j=1}^{N_r} j^2 VRLM(i,j) / \sum_{i=1}^{N_g} \sum_{j=1}^{N_r} VRLM(i,j)$
- Gray Level Nonuniformity: $f_3 = \sum_{i=1}^{N_g} (\sum_{j=1}^{N_r} VRLM(i,j))^2 / \sum_{i=1}^{N_g} \sum_{j=1}^{N_r} VRLM(i,j)$
- Run Length Nonuniformity: $f_4 = \sum_{j=1}^{N_g} (\sum_{i=1}^{N_r} VRLM(i,j))^2 / \sum_{i=1}^{N_g} \sum_{j=1}^{N_r} VRLM(i,j)$
- Run Percentage: $f_5 = \sum_{i=1}^{N_g} \sum_{j=1}^{N_r} VRLM(i,j) / VRLM$

In addition, emphasis features are used [11]. The following mentions the feature functions:

| | | Actual | | Total |
|---|---|---|---|---|
| | | AMD | Not AMD | |
| Predicted | AMD | 15 | 3 | 18 |
| | Not AMD | 0 | 7 | 7 |
| Total | | 15 | 10 | 25 |

Table 2. The truth table showing the result.

- Low Gray-Level Run Emphasis: $f_6 = \frac{1}{N_r} \sum_{i=1}^{N_g} \sum_{j=1}^{N_r} \frac{VRLM(i,j)}{i^2}$
- High Gray-Level Run Emphasis: $f_7 = \frac{1}{N_r} \sum_{i=1}^{N_g} \sum_{j=1}^{N_r} VRLM(i,j) \cdot i^2$

More features are extracted using the emphasis [12]. The following functions explain how the feature elements are extracted:

- Short Run Low Gray-Level Emphasis: $f_8 = \frac{1}{N_r} \sum_{i=1}^{N_g} \sum_{j=1}^{N_r} \frac{VRLM(i,j)}{i^2 \cdot j^2}$
- Short Run High Gray-Level Emphasis: $f_9 = \frac{1}{N_r} \sum_{i=1}^{N_g} \sum_{j=1}^{N_r} \frac{VRLM(i,j) \cdot i^2}{j^2}$
- Long Run Low Gray-Level Emphasis: $f_{10} = \frac{1}{N_r} \sum_{i=1}^{N_g} \sum_{j=1}^{N_r} \frac{VRLM(i,j) \cdot j^2}{i^2}$
- Long Run High Gray-Level Emphasis: $f_{11} = \frac{1}{N_r} \sum_{i=1}^{N_g} \sum_{j=1}^{N_r} VRLM(i,j) \cdot i^2 \cdot j^2$

The identified features were used to describe a feature vector.

## 3. CLASSIFICATION

The feature vectors, derived as described above, and coupled with an appropriate class label are used as input to a classifier generator. The k-Nearest Neighbor (KNN) classifier was used [13]. Two classes were used for the training: normal retina and AMD retina. For the VCM, 22 features were computed for each of the 13 matrices giving feature vectors comprising 286 features (one per image). For the case of the VRLM, 11 features were calculated giving 143 features.

## 4. DISCUSSION

The first advantage offered by the matrix method described is that it does not required any segmentation of the retina before computing the features. 3-D segmentation remains a subject of much research, and remains a challenge because of the computational complexity that 3-D segmentation entails.

To evaluate the effectiveness of the proposed approach we have run experiments using 25 3D OCT volumes, ten "normal" and the remainder AMD. Each volume has different sizes according to the size of the retina. In most cases, the size is about $(596 \times 465\ pixels) \times 18\ slices$. Some image enhancement was firs applied using a global threshold and morphological operations. Then the FVs were extracted and input to a KNN classifier. The entire data set was used to build the classifier which was then tested on the same data (alternatives might have been to use ten cross validation or a "leave one out" approach). The resulting truth table is presented in Table 2. From the truth table we get the following results: sensitivity = 100%, specificity = 70% and accuracy = 88%. These are good results although an argument can be made that the classifiers is over-fitted to the data. However, we can conclude that the second advantage offered by the matrix method is that it maintains the spatial relationships between the features even when the shape is rotated and transformed thus obviating the need for the implementation of some flatten process as suggested in [2].

## 5. CONCLUSION AND FUTURE WORK

We have given a brief overview of the Voxel Co-occurrence Matrix (VCM) and Voxel Run-Length Matrix (VRLM) methods for building shape descriptors for image classification purposes. Although this is work in progress, preliminary experiments have demonstrated that the feature extracted should allow a classifier to distinguish between normal and AMD 3-D retinal images. It is conjectured that the combination of the features will heighten accuracy. For future work we intend improve the manner in which the matrices are constructed. The intention is also to add more features so as to enhance accuracy. Furthermore, the total number of features could be normalized in a way that takes 13 vectors in consideration and in the same time one value is used instead of 13. Alternatively dimensionality reduction method such as Principal Component Analysis (PCA) may be used instead.

## REFERENCES


[1] Huang, D., Swanson, E., Lin, C., Schuman, J., Stinson, W., Chang, W., Hee, M., Flotte, T., Gregory, K., Puliafito, C., and et, a., "Optical coherence tomography," *Science* **254**(5035), 1178–1181 (1991).

[2] Liu, Y.-Y., Chen, M., Ishikawa, H., Wollstein, G., Schuman, J. S., and Rehg, J. M., "Automated macular pathology diagnosis in retinal oct images using multi-scale spatial pyramid and local binary patterns in texture and shape encoding," *Medical Image Analysis* **In Press, Corrected Proof** (2011).

[3] Haralick, R. M., Shanmugam, K., and Dinstein, I., "Textural features for image classification," *Systems, Man and Cybernetics, IEEE Transactions on* **3**(6), 610–621 (1973).

[4] Gao, D., "Volume texture extraction for 3d seismic visualization and interpretation," *Geophysics* **68**(4), 1294–1302 (2003).

[5] Chen, W., Giger, M. L., Li, H., Bick, U., and Newstead, G. M., "Volumetric texture analysis of breast lesions on contrast-enhanced magnetic resonance images," *Magnetic Resonance in Medicine* **58**(3), 562–571 (2007).

[6] Kim, J. K. and Park, H. W., "Statistical textural features for detection of microcalcifications in digitized mammograms," *Medical Imaging, IEEE Transactions on* **18**, 231 –238 (Mar 1999).

[7] Clausi, D. A., "An analysis of co-occurrence texture statistics as a function of grey level quantization," *Canadian Journal of Remote Sensing* **28**(1), 45–62 (2002).

[8] Soh, L.-K. and Tsatsoulis, C., "Texture analysis of sar sea ice imagery using gray level co-occurrence matrices," *Geoscience and Remote Sensing, IEEE Transactions on* **37**, 780 –795 (Mar 1999).

[9] Galloway, M. M., "Texture analysis using gray level run lengths," *Computer Graphics and Image Processing* **4**(2), 172 – 179 (1975).

[10] Tang, X., "Texture information in run-length matrices," *Image Processing, IEEE Transactions on* **7**, 1602 –1609 (Nov 1998).

[11] Chu, A., Sehgal, C. M., and Greenleaf, J. F., "Use of gray value distribution of run lengths for texture analysis," *Pattern Recogn. Lett.* **11**, 415–420 (Jun 1990).

[12] Dasarathy, B. V. and Holder, E. B., "Image characterizations based on joint gray level-run length distributions," *Pattern Recogn. Lett.* **12**, 497–502 (Aug 1991).

[13] Fix, E. and Hodges, J. L., J., "Discriminatory analysis. nonparametric discrimination: Consistency properties," *International Statistical Review / Revue Internationale de Statistique* **57**(3), pp. 238–247 (1989).